netic field values corresponding to the maxima of THG and those corresponding to the transmission minima requires more theoretical work about the details of nonlinear dispersion at frequencies larger than the band gap.

We would like to thank S. J. Buchsbaum and P. A. Wolff for helpful comments on the manuscript, J. W. Klüver for help in the 3.508-μ transmission measurements, and Victor C. Wade for his skillful preparation of the thin samples.

[1]C. K. N. Patel, P. A. Fleury, R. E. Slusher, and H. L. Frisch, Phys. Rev. Letters 16, 971 (1966).

[2]K. J. Button, Benjamin Lax, Margaret H. Weiler, and M. Reine, Phys. Rev. Letters 17, 1005 (1966).

[3]C. K. N. Patel, R. E. Slusher, and P. A. Fleury, Phys. Rev. Letters 17, 1011 (1966).

[4]P. A. Wolff and G. A. Pearson, Phys. Rev. Letters 17, 1015 (1966).

[5]B. Lax, W. Zawadzki, and M. H. Weiler, Phys. Rev. Letters 18, 462 (1967).

[6]Equation (1) applies only to the case in which the interband transition involves Landau levels having the same quantum number n.

[7]All the data shown in Fig. 2 are obtained using a linearly polarized fundamental beam. We find that there is no observable THG when the fundamental beam is circularly polarized. This result is to be expected if the isotropic model for the band structure is used to calculate the third-order nonlinear susceptibility.

[8]C. R. Pidgeon and R. N. Brown, Phys. Rev. 146, 575 (1966).

[9]G. G. MacFarlane, T. P. McLean, J. E. Quarrington, and V. Roberts, Phys. Rev. Letters 2, 252 (1959).

[10]N. Bloembergen and P. S. Pershan, Phys. Rev. 128, 606 (1962).

[11]R. A. Soref, Stanford Electronics Laboratory, Stanfor University, Technical Report No. 0556-8, 1963 (unpublished).

GRAPHITE TRIPLE POINT AND SOLIDUS-LIQUIDUS INTERFACE EXPERIMENTALLY DETERMINED UP TO 1000 atm*

Glen J. Schoessow
University of Florida, Gainesville, Florida
(Received 29 July 1968)

The triple-point pressure of four grades of graphite was determined to be 103 atm (absolute). The triple-point temperature varied from one grade to another with values ranging from 4183 ± 10 to 4299 ± 25°K. The solidus-liquidus temperature measured for one grade increased with increasing pressure from 4247°K at 103 atm to 4306°K at 1000 atm.

The theoretical development of the graphite (carbon) phase diagram is receiving serious attention by this author and others; but until the theoretical results are more fruitful, the need for accurate experimental data is urgent.

The rapidly expanding use of graphite as a structural and ablative material for extreme high-temperature applications such as re-entry vehicles, supersonic-airplane leading edges, nuclear-rocket reactor and power reactor cores, etc., is making it essential to have accurate pressure-temperature phase-diagram data up to 1000 atm.

Graphite pressure-temperature phase-diagram research is made difficult by the normally noncompatible requirements of simultaneously maintaining high pressure and temperature for a test specimen. Investigators seeking experimental data on the graphite melting temperature are faced with many difficulties. Several approaches have been tried by Bassett,[1] Jones,[2] Noda,[3] Bundy,[4] and Fateeva[5] in order to maintain the desired environment and to accurately measure the melting temperature.

A test specimen large enough to make its own crucible provided the unique feature which allowed this work to achieve accurate results. The 11.5-mm-diam specimen was melted at the axial center line by electrical resistance heating, but remained solid at the outside surface at the time the melt temperature was achieved. A radial hole to the melt location provided an almost ideal blackbody cavity for the optical readings, thus eliminating the usual emissivity correction problem. A blackbody-calibrated monochromatic pyrometer was used for all temperature measurements. This pyrometer was calibrated by the National Bureau of Standards. Additional checks of the calibration were performed on the actual experimental setup by measuring the melting point of gold, molybdenum, and tungsten. The results of these tests verified the accuracy

of the pyrometer as it was used on this particular apparatus and indicated that the temperatures reported are very close to absolute values. Any required corrections to the readings were made in accordance with proved and accepted methods.[6]

In addition to the advantages of a large specimen, the accuracy was improved by the procedures used in the present work which eliminate or greatly reduce the sources of error present in some of the works referenced above. Helium gas was used to pressurize the test cell shown in Fig. 1. It was found by experiment that helium gas was much better than argon, used by the investigators referenced above. The pyrometer image was more stable and more clearly defined, especially at high temperature, when using helium. An optical tunnel was used from the specimen to the cell window to prevent specimen image distortion at the higher pressures.

The proper use of a ventilating hole, axial hole, hole plug at top of specimen, etc., helped greatly to eliminate the effects of a carbon vapor cloud which, if present, would degrade the temperature readings. Those same features also helped to insure that the cell pressure was indeed the pressure at the melt surface on the axis of the specimen.

The geometry of the specimen was arrived at after much experimenting. The small groove around the outside of the specimen (see Fig. 2) helped to concentrate the power at the point of interest and allowed temperature measurements to be obtained without vapor cloud problems right up to the melting-temperature value.

The necessary evidence for melting was taken to be the coincident presence of a dendritic-appearing melted region and/or of spheres of graphite which form from the melted phase (due to the action of surface tension on a liquid), and the rapid voltage rise across the specimen which results from an increase in specimen electrical resistance upon initiation of a phase change (e.g., melting or sublimation).

Three grades of graphite commercially available from Union Carbide Company, AGOT, AGSR, and AGKS, and one grade of special graphite, LANG, supplied by Los Alamos Scientific Labo-

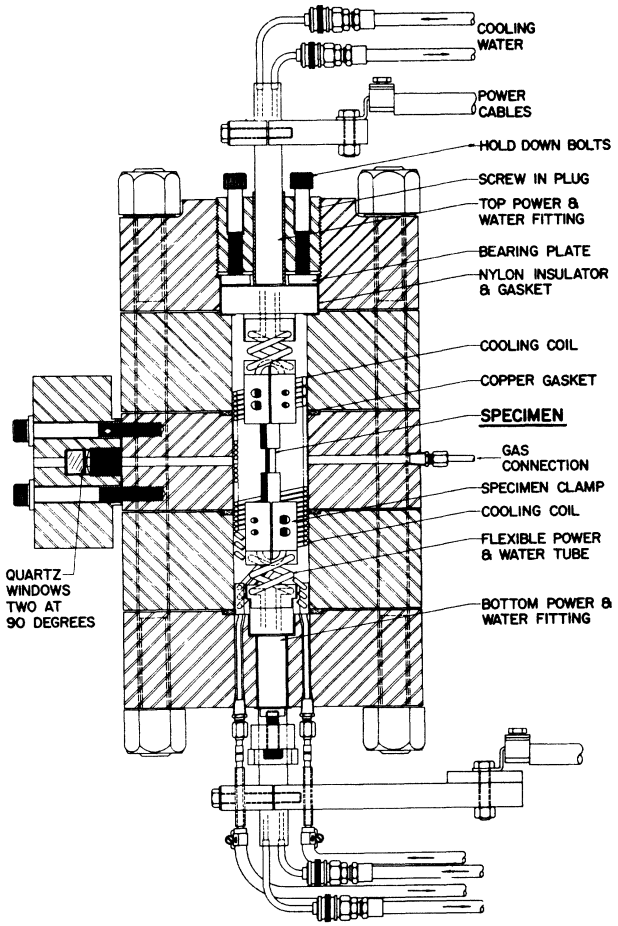

FIG. 1. Pressure-temperature test cell.

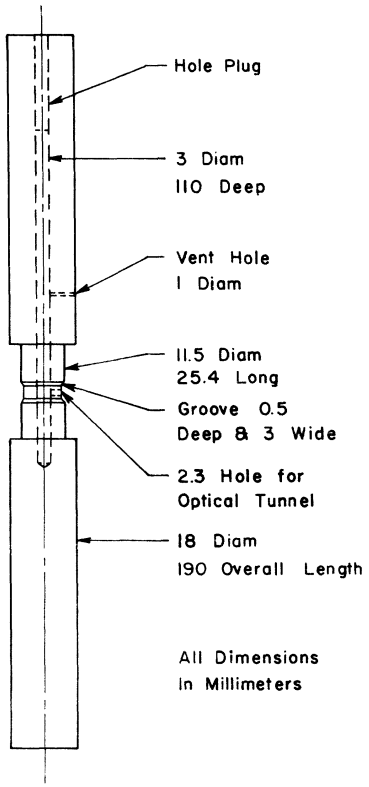

FIG. 2. Details of test specimen.

ratory, were selected for the program. Details of the LANG grade are given below; details of the other grades are available from the manufacturer. The LANG grade contained 70 ppm U^{235} and other minor impurities. It was manufactured from 60-mesh high-purity graphite flour base mixed with Thermax submicron carbon-black particles and a small amount of 40- to 50-mesh pine-wood flour. A partially polymerized furfuryl alcohol called Varcum 8251 was used as the binder. After blending, the above materials were extruded. Four thermal cycles were performed on the extrusion for a combined heat-up time of 127 h. The final operation was graphitization at 2620°K for four hours.

Three kinds of experiments, as described below, were conducted to acquire the data shown in Fig. 3. These were triple-point pressure tests, triple-point temperature tests, and melting-temperature tests from 200 to 1000 atm.

The triple-point pressure was located by conducting experiments at various pressures above and below 100 atm, and then visually examining the sectioned specimen under a 120× microscope. The specimen geometry used for these tests is shown in Fig. 2 except that the hole plug and vent hole shown were not added until tests above the triple-point pressure. This geometry was necessary to insure that melting occurred under a known pressure. If the holes had not been present or if they had become plugged during a test, any melting observed inside the specimen occurred under the measured gas pressure plus an unknown pressure from restrained thermal expansion. All tests reported herein were terminated with the radial and axial holes still open to provide pressure relief. The triple-point pressure for four grades of graphite was determined to be 103 atm.

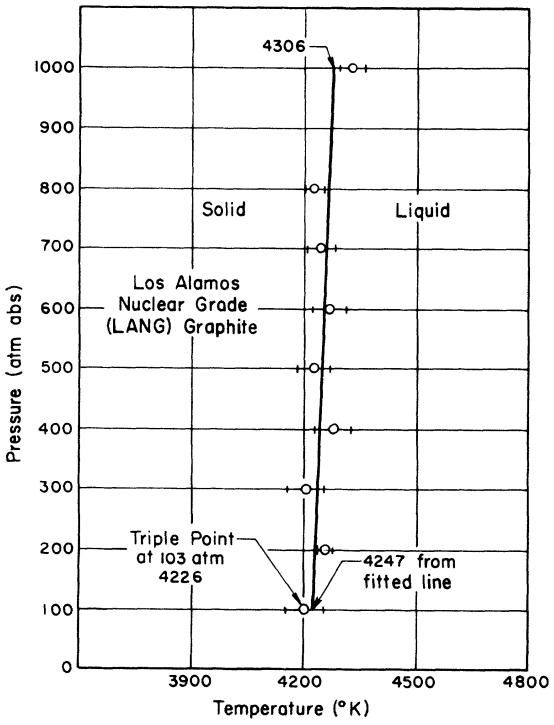

FIG. 3. Pressure-temperature phase diagram for LANG-grade graphite up to 1000 atm.

The triple-point temperature tests used the same specimen geometry as the triple-point pressure tests described above. The radial-hole, axial-hole combination formed a vent system which served to sweep away much of the otherwise troublesome graphite vapor. During some tests, small amounts of a dark-appearing vapor would be observed in the radial hole during the highest temperature measurements. This vapor would absorb some of the emerging blackbody radiations thus lowering the readings and eventually partially plugging the radial hole. The readings thus affected are not included in the data. After the dark vapor appeared, the power increase was allowed to continue until a rapid rise in voltage was taken as the melting initiation power. The central cavity temperature was calibrated against power at temperatures below the threshold for significant amounts of carbon vapor. The calibration, together with the accurately measured power at which melting began, was then used to extrapolate the last several hundred degrees to the melting temperature for some tests by using an appropriate equation and a least-squares technique. Use of these procedures largely eliminated the effects of carbon vapor on the measurements. The triple-point temperature results are the following: 4183 ± 10°K for AGOT, 4226 ± 33°K for LANG, 4238 ± 18°K for AGSR, and 4299 ± 25°K for AGKS. These values are the mean value plus or minus one standard deviation of the mean. Five or more specimens were tested for each grade to establish the mean value and the deviation.

The results obtained for the melting temperature of LANG-grade graphite for pressures of 200 through 1000 atm are given in Fig. 3. Five or more specimens were tested at each pressure to establish the deviation shown in Fig. 3.

A linear least-squares fit to the solidus-liquidus interface data from 200 to 1000 atm for LANG grade predicts 4247°K which is in excellent

agreement with the 4226°K mean triple-point temperature measured for LANG-grade graphite as shown in Fig. 3. This agreement provides a verification of the triple-point temperature of LANG-grade graphite.

*Work supported by the National Aeronautics and Space Administration Lewis Research Center.

[1]J. Bassett, J. Phys. Radium 10, 217 (1939).
[2]M. T. Jones, National Carbon Research Laboratories Report No. PRC-3, 1958 (unpublished).
[3]T. Noda, in Proceedings of an International Symposium on High Temperature Technology, Asilomar, California, 6-9 October 1959 (McGraw-Hill Book Company, Inc., New York, 1960).
[4]F. P. Bundy, J. Chem. Phys. 38, 618 (1963).
[5]N. I. Fateeva et al., Dokl. Akad. Nauk SSSR 152, 88 (1963) [translation: Soviet Phys.—Doklady 8, 893 (1964)].
[6]H. J. Kostkowski and R. D. Lee, Theory and Methods of Optical Pyrometry, National Bureau of Standards Monograph No. 41 (U. S. Government Printing Office, Washington, D. C., 1962).

STATISTICAL MODEL FOR A DZIALOSHINSKII FERROMAGNET*

C. W. Searle
Department of Physics, University of Manitoba, Winnipeg, Canada
(Received 22 July 1968)

Arguments are developed to show that the Dzialoshinskii vector $\vec{D}$ should be calculated according to statistical mechanics.

In molecular field calculations the term

$$\vec{D}\cdot(\vec{M}_1\times\vec{M}_2) \tag{1}$$

is usually introduced to describe the Dzialoshinskii-Moriya interaction for those antiferromagnets which exhibit this type of weak ferromagnetism. $\vec{M}_1$ and $\vec{M}_2$ are the sublattice magnatizations and $\vec{D}$ is assumed to be a constant vector. In hematite, which will be used throughout as a typical example, $\vec{D}$ is parallel to the [111] crystallographic direction.

It is the purpose of this Letter to show that $\vec{D}$ should not be treated as a constant vector but should be calculated according to statistical mechanics.

The notation used by Dzialoshinskii[1] will be used to express the thermodynamic potential Φ. In this notation $\vec{m}=\vec{s}_1+\vec{s}_2+\vec{s}_3+\vec{s}_4$, and $\vec{l}=\vec{s}_1-\vec{s}_2-\vec{s}_3+\vec{s}_4$. The vector $\vec{m}$ is the mean magnetic moment of the unit cell, and each $\vec{s}$ is the mean magnetic moment per ion, while the subscripts indicate the relative location of each magnetic ion along the [111] direction of the unit cell. The antiferromagnetic ordering of the magnetic moments in hematite is $\vec{s}_1=-\vec{s}_2=-\vec{s}_3=\vec{s}_4$ when only isotropic exchange is considered. The most general form for the expansion of Φ, to second order, consistent with the symmetry of the crystal and the relative antiferromagnetic ordering of the spins is

$$\Phi_{\pm}=\tfrac{1}{2}Al^2+\tfrac{1}{2}Bm^2+\tfrac{1}{2}\alpha l_z^{\,2}+\tfrac{1}{2}bm_z^{\,2}\pm\beta(l_xm_y-l_ym_x)+\tfrac{1}{4}Cl^4. \tag{2}$$

The first two terms and the last one are exchange energies, the third and fourth terms are anisotropy energies, and the "mixed" term of the form $l_xm_y-l_ym_x$ leads to the possibility of a weak spontaneous moment.[1] Since the "mixed" term satisfies all symmetry requirements, then any term formed by multiplying this "mixed" term by a constant also satisfies all symmetry requirements. This fact is emphasized by requiring β to be a positive constant multiplied by ±1, or simply $\pm\beta$. Φ_+ corresponds to $+\beta$ while Φ_- corresponds to $-\beta$. The solution of the equations which provide the minimum Φ yields the following results:

$$\text{(I)}\ \vec{m}=0,\ l_x=l_y=0;$$

$$\text{(II)}_+\ l_z=0,\ m_z=0,\ m_x=(\beta/B)l_y,\quad m_y=-(\beta/B)l_x;$$

and

$$\text{(II)}_-\ l_z=0,\ m_z=0,\ m_x=-(\beta/B)l_y,\quad m_y=(\beta/B)l_x. \tag{3}$$

State (I) corresponds to the low-temperature configuration and will not be considered further. States $(\text{II})_+$ and $(\text{II})_-$ correspond to possible configurations in the temperature range between T_M, the Morin transition, and T_N, the Néel temperature. Both states $(\text{II})_+$ and $(\text{II})_-$ have a spontaneous magnetic moment, however, $\vec{m}_+$